Immunity
Resource

Network Analysis Reveals Centrally Connected Genes and Pathways Involved in CD8+ T Cell Exhaustion versus Memory

Travis A. Doering,[1,2] Alison Crawford,[1,3] Jill M. Angelosanto,[1] Michael A. Paley,[1] Carly G. Ziegler,[1] and E. John Wherry[1,*]
[1]Department of Microbiology and Institute for Immunology, Perelman School of Medicine, University of Pennsylvania, Philadelphia, PA 19104, USA
[2]Present address: Hofstra North Shore-LIJ School of Medicine, Hempstead, NY 11549, USA
[3]Present address: Regeneron Pharmaceutical, Tarrytown, NY 10591, USA
*Correspondence: wherry@mail.med.upenn.edu
http://dx.doi.org/10.1016/j.immuni.2012.08.021

SUMMARY

Exhausted CD8+ T cells function poorly and are negatively regulated by inhibitory receptors. Transcriptional profiling has identified gene expression changes associated with exhaustion. However, the transcriptional pathways critical to the differences between exhausted and functional memory CD8+ T cells are unclear. We thus defined transcriptional coexpression networks to define pathways centrally involved in exhaustion versus memory. These studies revealed differences between exhausted and memory CD8+ T cells including the following: lack of coordinated transcriptional modules of quiescence during exhaustion, centrally connected hub genes, pathways such as transcription factors, genes involved in regulation of immune responses, and DNA repair genes, as well as differential connectivity for genes including T-bet, Eomes, and other transcription factors. These data identify pathways involved in CD8+ T cell exhaustion, and highlight the context-dependent nature of transcription factors in exhaustion versus memory.

INTRODUCTION

During acute viral infections, naive CD8+ T cells differentiate into effector CD8+ T cells and, after viral control, into memory CD8+ T cells. Memory CD8+ T cells are highly functional, proliferate rapidly upon reinfection, and persist long-term without antigen (Williams and Bevan, 2007). In contrast, during chronic infections, CD8+ T cells become "exhausted" and have poor effector function, express multiple inhibitory receptors, possess low proliferative capacity, and cannot persist without antigen (Wherry, 2011). Though first observed in lymphocytic choriomeningitis virus (LCMV) infection in mice, CD8+ T cell exhaustion is a prominent feature of many experimental models of chronic infections, as well as in humans with chronic infections and cancer, and this dysfunction prevents optimal control of infections and tumors in these settings (Wherry, 2011).

Despite the importance of CD8+ T cell exhaustion during persisting infections, the underlying molecular mechanisms remain incompletely understood. Recent studies suggest that T cell exhaustion is orchestrated, at least in part, by regulation via inhibitory cell surface receptors (e.g., PD-1, Lag-3, Tim-3, and others) and soluble mediators, such as IL-10 and TGF-β (Wherry, 2011). These observations demonstrate that T cell exhaustion is part of an active negative regulatory process and is not simply a passive, intrinsic failure to recognize or respond to infection. The existence of active regulatory pathways highlights the possibility of restoring function to exhausted T cells, with clear clinical implications. Indeed, early clinical trials blocking the PD-1 pathway show promise against cancer (Brahmer et al., 2012; Topalian et al., 2012).

However, functional alterations in exhausted CD8+ T cells extend beyond inhibitory receptors and immunoregulatory pathways. Previous transcriptional profiling studies have demonstrated profound changes in metabolism, cell cycle regulation, and transcription factor expression (Wherry et al., 2007). Thus, two major questions emerge: (1) what is the underlying transcriptional program of exhausted CD8+ T cells, and (2) can knowledge of this transcriptional program be used to identify genes, groups of genes, and pathways central to the differential development of CD8+ T cell memory versus exhaustion?

Transcriptional profiling is a powerful tool that has been used to examine several aspects of CD8+ T cell differentiation (Kaech et al., 2002; Hertoghs et al., 2010; Wherry et al., 2007; Wirth et al., 2010). These and other studies used gene-centric, fold-change-based approaches to focus on the implications of expression differences between individual genes. More recent studies have applied increasingly integrated methods to harness the power of combining data sets across cell types and species (Quigley et al., 2010). As the technologies for high-throughput genomics become more efficient and accessible, it has become possible to expand the use of transcriptional profiling to define "networks" of transcriptional interactions. Such networks have identified groups of coordinately expressed genes involved in disease (Chaussabel et al., 2008), hematopoietic lineage differentiation (Ng et al., 2009; Novershtern et al., 2011), and T cell differentiation (Elo et al., 2007). Several major advantages of transcriptional coexpression networks make such studies a next step in the genomic understanding of T cell memory and exhaustion. First, compared to previous studies, transcriptional network analysis is less dependent on the magnitude of change in expression of any individual gene (Carter et al., 2004). Network analysis allows connections between genes and pathways to be

revealed that might otherwise have been unappreciated (Dong and Horvath, 2007). Second, network analysis reveals genes and pathways that are predicted to be central to the biological system being analyzed because highly connected "hub" genes represent likely control points (Carter et al., 2004; Han et al., 2004; Jeong et al., 2001). Finally, network analysis identifies modules of highly correlated genes representing transcriptional developmental programs that might be combined and reused in different ways to generate cells with distinct properties or fates (Novershtern et al., 2011). Thus, transcriptional coexpression networks can allow for a deeper understanding of complex cellular systems.

Using the well-defined LCMV system, we have addressed key questions about the differentiation of memory versus exhausted $CD8^+$ T cells by defining modular transcriptional networks of coexpressed genes. This approach demonstrated that $CD8^+$ T cell memory and exhaustion reflect distinct states defined by coordinated sets of modules. Furthermore, this analysis revealed several observations about exhausted CD8 T cells. First, exhausted $CD8^+$ T cells lacked modules associated with quiescence. Additionally, altered connectivity of key negative regulators in exhausted $CD8^+$ T cells was associated with a prolonged activation program that could be distinguished from a prolonged effector program. Specific genes and pathways differentially implicated in exhaustion versus memory were identified including genes involved in epigenetics, DNA damage, and WNT signaling, and specific genes including: *Rtp4*, *Foxp1*, *Ikzf2*, *Zeb2*, *Lass6*, *Tox*, and *Eomes*. Finally, network analysis revealed context-specific connectivity patterns for key transcription factors, including T-bet, demonstrated by largely nonoverlapping sets of functionally distinct "neighbor" genes (genes closely connected in the correlation-based network) in exhausted versus memory $CD8^+$ T cells. These studies reveal insights into the biology of exhausted $CD8^+$ T cells and provide a resource that should allow for deeper understanding of $CD8^+$ T cell differentiation following acute and chronic viral infection.

RESULTS

Scale-free Transcriptional Networks for $CD8^+$ T Cells in Acute versus Chronic Viral Infection

$CD8^+$ T cell exhaustion develops during chronic infections and cancer and prevents optimal control of infections and tumors (Wherry, 2011). Previous transcriptional profiling studies have defined specific genes involved in exhausted versus functional effector and memory $CD8^+$ T cells (Wherry et al., 2007). Computational approaches, including modular transcriptional networks, can provide insight into the regulation of cellular differentiation and control of cellular processes (Zhang and Horvath, 2005) but require more extensive sets of transcriptional data than previously available for exhausted $CD8^+$ T cells. Thus, we performed longitudinal transcriptional profiling of virus-specific $CD8^+$ T cells through acutely resolved and chronic LCMV infection. Infection of adult C57BL/6 mice with the LCMV Armstrong (Arm) strain causes an acute infection that is cleared by d8–d10 postinfection (p.i.) and results in functional effector and memory $CD8^+$ T cells. Infection with LCMV clone 13, however, causes a chronic infection resulting in $CD8^+$ T cell exhaustion (Wherry et al., 2003). Exhausted $CD8^+$ T cells are characterized by progressive and hierarchical loss of effector functions and ineffective viral control (Fuller and Zajac, 2003; Wherry et al., 2003). To begin to define the organization of transcriptional networks associated with either $CD8^+$ T cell memory or exhaustion, we sorted naive $CD44^{lo}$ $CD8^+$ T cells and $CD8^+$ T cells specific for the LCMV epitope D^bGP33 on d6, d8, d15, or d30 p.i. with LCMV Arm or clone 13 (Figure 1A). Following LCMV Arm infection, virus-specific $CD8^+$ T cells initially were $CD127^{lo}$ and $PD\text{-}1^+$ (Figure 1A). Expression of PD-1 declined and CD127 increased over time as memory $CD8^+$ T cells developed following acute infection (Figure 1A). During LCMV clone 13 infection, the initial pattern of CD127 and PD-1 expression was similar to Arm infection, but CD127 remained low and the expression of PD-1 further increased as these cells became exhausted (Figure 1A; Wherry et al., 2007). Following LCMV Arm infection, virus-specific $CD8^+$ T cells remained highly functional, whereas during chronic infection these cells lost the ability to coproduce cytokines (data not shown; Fuller and Zajac, 2003; Wherry et al., 2003).

We profiled global messenger RNA (mRNA) expression from naive $CD8^+$ T cells and $H\text{-}2D^b$ GP33-specific $CD8^+$ T cells using Affymetrix microarrays on d6, d8, d15, and d30 following acute or chronic infection. Initial analysis of differentially expressed genes, ranked by the signal to noise ratio, revealed distinct groups corresponding to different stages of the immune response (Figure 1B). These gene expression profiles highlight the similarity during early LCMV Arm and clone 13 infections (black bars in Figure 1B), consistent with the similar functional profiles during the first week of infection (Fuller and Zajac, 2003; Wherry et al., 2007). As memory and exhausted $CD8^+$ T cells developed following acutely resolved versus chronic infection, there was a progressive divergence of transcriptional profiles. This divergence occurred between d8–d30 p.i. and is consistent with previous studies indicating more similarity in the $CD8^+$ T cell response to LCMV Arm and clone 13 at early time points p.i. (Brooks et al., 2006; Fuller and Zajac, 2003; Wherry et al., 2003, 2007; Angelosanto et al., 2012).

To obtain a more global view of the transcriptional changes in the $CD8^+$ T cell response to acute or chronic LCMV, we used gene coexpression networks to identify transcriptional modules representing distinct patterns of gene expression (Dong and Horvath, 2007). Gene modules can function as conserved molecular "circuits" responsible for specific cellular functions that can be reused in different cell lineages (Novershtern et al., 2011). Though transcriptional networks are, by definition, based on correlations between the expression profiles of individual genes, highly correlated genes often share important biological features such as involvement in common cellular processes or similar mechanisms of regulation (Brown and Botstein, 1999). Here we used Pearson's correlation coefficient to define coexpression relationships between all pairs of genes in our transcriptional data sets. These correlations establish a network of interconnected genes based on the strength of connections (i.e., correlation coefficient) between all pairs of genes. Strong relationships identify closely "neighboring" genes and areas within a network where a high density of genes share strong relationships to one another are termed modules. Within each module, highly connected "central" genes are called hubs. Genes in modules often share common regulatory mechanisms

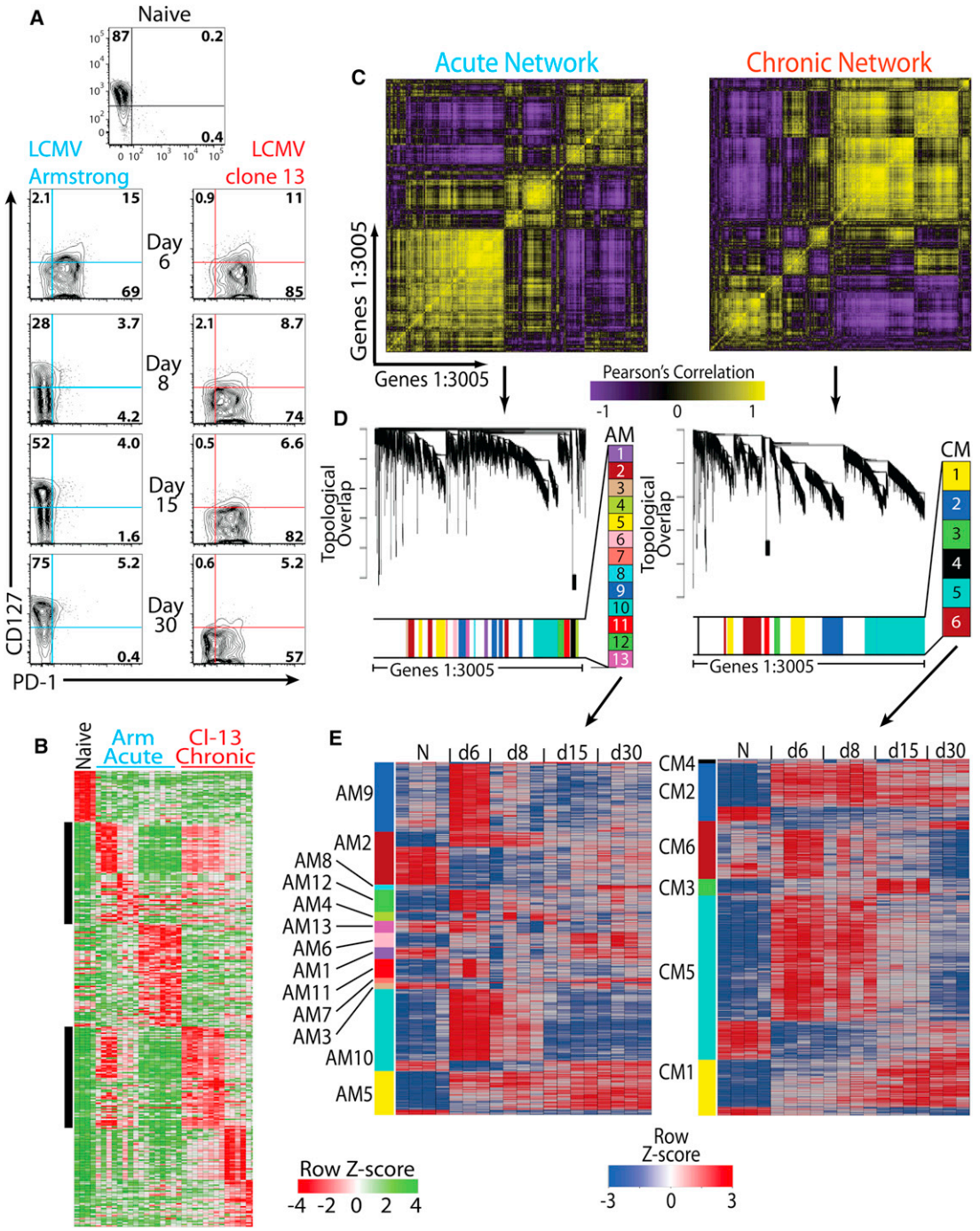

Figure 1. Characterization of Effector, Memory, and Exhausted LCMV-Specific CD8$^+$ T Cells

(A) Naive CD8$^+$ CD44^{lo} and H2-Db GP33 tetramer$^+$ CD8$^+$ T cells were sorted at d0 and d6, d8, d15, and d30 p.i., respectively. Representative expression of CD127 and PD-1 at these time points is shown.

(B) Global mRNA expression profiles of naive and effector, memory, and exhausted CD8$^+$ T cells from acutely resolved and chronic LCMV infection. The top 25 most differentially expressed genes at each time point were identified. Black bars mark effector-biased genes. Green and red represent low and high relative expression, respectively.

(C) Gene coexpression network construction was performed. Pearson's correlation between the expression profiles of each pair of genes, for both all naive and acute arrays (left) and also across all naive and chronic arrays (right), were hierarchically clustered and visualized as heatmaps. Positive correlations are yellow and negative correlations purple.

(D) Coexpression module identification. Highly coexpressed modules were defined (see Experimental Procedures).

(E) Genes of each module were hierarchically clustered and expression levels were plotted as heatmaps; blue indicates low relative expression and red high relative expression.

or are involved in related cellular functions. Moreover, hub genes can function as key control points in the formation of modules and the cellular functions they confer.

We generated two coexpression networks from virus-specific $CD8^+$ T cells: one from acutely resolved LCMV infection (LCMV Arm) and one from chronic LCMV infection (LCMV clone 13), as described (Zhang and Horvath, 2005), Figure 1C). Within these networks we identified densely interconnected regions, or modules, based on the topological overlap (TO), a network metric that determines the proportion of highly coexpressed neighbors common between two genes (Yip and Horvath, 2007). Modules are displayed here by color and number, though color and number do not imply module similarity between the acute and chronic networks (see below). Modules identified by this method ranged from 20 to 776 genes (see Table S1 available online). These modules encompassed a variety of patterns when the expression of the individual genes in each module was viewed over time (Figure 1E). Note that the Pearson's correlation-based approach used here depends on coordinated changes in expression, but not the direction of that change. To define statistical differences in temporal expression of modules, we performed a one-way ANOVA between d6 and 30 (Figure S1A). Several modules in each network (e.g., AM9-AM13, CM2, and CM5) display expression profiles biased toward effector time points, consistent with the widespread changes in gene expression as naive $CD8^+$ T cells become activated. Also common to both networks were late-biased modules (AM5, AM6, AM7, AM8, and CM1), implying a possible role in the differentiation programs of $CD8^+$ T cell memory or exhaustion. The remaining module expression patterns from both the acute and chronic networks suggest a complex transcriptional architecture underlying each response.

Transcriptional Module Differences and Similarities between Acute and Chronic Networks

To identify the degree of similarity between modules from the acute versus chronic network, we used Fisher's Exact Test (FET) (Figure 2A). With the exception of CM4, all modules of the chronic network had significant similarity to at least one module from the acute network. However, the converse was not true; multiple acute modules lacked a counterpart in the chronic network (i.e., AM1, AM3, AM7, AM8, AM11, and AM12). Thus, although previous studies have identified specific genes upregulated in exhausted $CD8^+$ T cells, including *Pdcd1* (PD-1), *Prdm1* (Blimp-1), and *Batf* (Barber et al., 2006; Quigley et al., 2010; Shin et al., 2009), this analysis revealed that a major feature of $CD8^+$ T cell exhaustion was the absence of key $CD8^+$ T cell memory-associated modules of gene expression.

To explore the characteristics of these modules in more detail, we compared their temporal expression profiles. The expression pattern of each module was summarized by its module eigengene (defined by the first principal component of gene expression [Langfelder and Horvath, 2007]). Modules with temporal similarity were grouped by hierarchical clustering based on Pearson's correlation coefficient between their module eigengenes (Figure 2B). Expression of the chronic-only module CM4 was highly biased to later time points. Acute modules absent from the chronic network (AM1, AM3, AM7, AM8, AM11, and AM12) were expressed at either effector (AM11 and AM12) or memory (AM7 and AM8) phases of the response (Figure S1). AM3 and AM1, the remaining two acute modules not preserved in the chronic network, fit a resting or quiescent profile with high expression in both naive and memory populations and included genes with potential roles in regulating T cell responses such as *Rictor*, *Cbl-b*, *Rasa1*, and *Apobec3* (full lists in Table S2). Notably, the chronic network lacked a quiescence module, suggesting that exhausted $CD8^+$ T cells subjected to persistent antigenic stimulation may be unable to "disarm" their activation state and return to homeostasis despite downregulating the effector-like modules CM5 and CM6 (Figure 2B).

We next identified centrally connected hub genes within each module. Though based on correlations, hub genes represent likely control points for biological processes (Carter et al., 2004; Jeong et al., 2001). These hubs are defined by their intramodular connectivity (i.e., degree of coexpression) between a gene and all other genes in the same module (Carlson et al., 2006). The top 25 hub genes for each module were examined using DAVID (Huang et al., 2009b) to detect over-represented gene ontology (GO) terms. Representative terms for each module are shown in Figure 2C (full list in Table S3). Effector biased modules in each network (AM9, AM10, AM11, AM12, AM13, CM2, and CM5) displayed concordant enrichment for genes involved in cell cycle, mitosis, DNA replication, and repair, and the immune response, all of which are consistent with the activated and highly proliferative state of effector $CD8^+$ T cells. Several memory and exhaustion-biased modules (AM5, AM6, and AM7; CM1 and CM3, respectively) were enriched for genes regulating apoptosis and programmed cell death, in addition to immune response genes. A highly exhaustion biased module, CM1, was also enriched for genes involved in Wnt pathway signaling, suggesting an previously unappreciated role for this pathway during $CD8^+$ T cell exhaustion. Thus, identification of hub genes through network analysis helps define key similarities and differences between pathways associated with development of functional CD8 T cell memory versus exhaustion.

Delayed Resolution of the Effector Circuitry during Chronic Infection

Many of effector-biased modules had a high degree of similarity to at least one module from the opposite network. For example, the robust preservation between AM10 and CM5 (Figure 2A, p value $< 10^{-298}$) suggests that similar transcriptional programs regulate DNA replication and the cell cycle during the periods of high $CD8^+$ T cell proliferation for both infections. AM5 and CM2 also have highly significant overlap (Figure 2A), driven, in part, by key effector genes such as granzyme A (*Gzma*), interferon-γ (*Ifng*), and perforin (*Prf1*). A key distinction between these and other effector modules in the acute and chronic networks is the duration that these modules were upregulated during chronic infection. Effector modules of the acute network (AM9, AM10, AM11, AM12, and AM13) began downregulation by d8 p.i., whereas chronic effector modules (CM2, CM5) remained elevated through d15 p.i. despite previous studies demonstrating similar kinetics and duration of the effector and contraction phases during acute and chronic viral infection (Badovinac et al., 2002; Wherry et al., 2007). One potential explanation for this difference is the persistence of antigen during chronic infection. However, the chronic network lacked a module equivalent

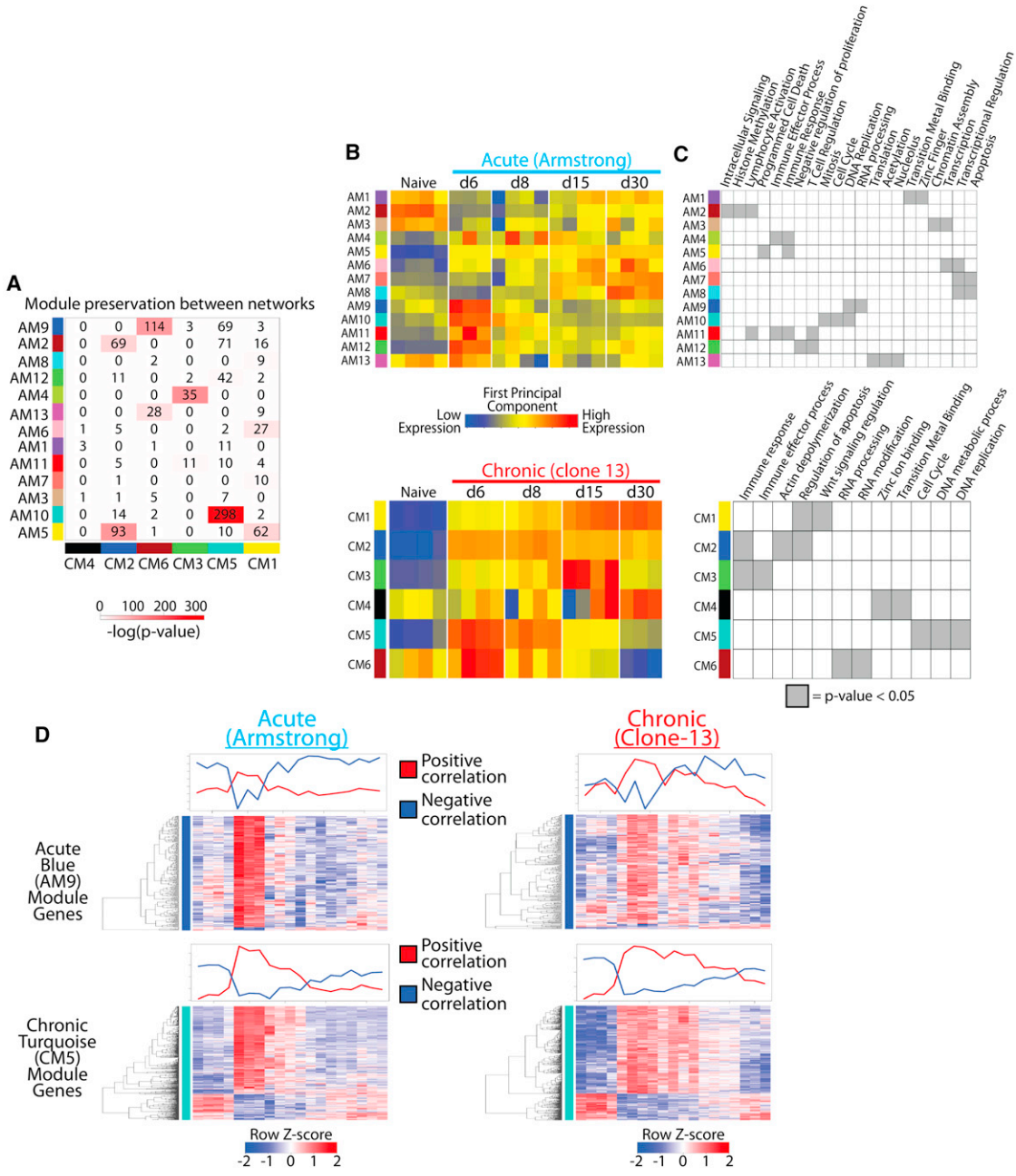

Figure 2. Modular Analysis of Acutely Resolved Versus Chronic CD8$^+$ T Cell Networks

(A) The number of genes in common between all pairings of acute and chronic modules was determined and Fisher's exact test used to calculate the significance of overlap. Darker red shading identifies more significant overlap. Genes from one module that were not contained in any module of the other network were excluded.

(B) Modules were clustered by Pearson's correlation coefficient between module eigengenes (ME) and visualized as heatmaps. Blue and red represent low and high relative expression, respectively.

(C) The top 25 hub genes for each module were identified by their intramodular connectivity, and overenriched GO (http://www.geneontology.org) terms were examined using DAVID (http://david.abcc.ncifcrf.gov/). Grey shaded boxes represent modules with significant enrichment (p value < 0.05; Table S3).

(D) The expression of AM9 and CM5, effector-biased modules from each network, was plotted for both the acute and chronic arrays. Blue and red represent low and high relative expression, respectively. Each gene was correlated with the module eigengenes of AM9 and CM5 and, above each heatmap; average expression of positively and negatively correlated genes was plotted in red and blue, respectively.

to AM12, which contains genes involved in regulation of T cell activation and includes the hub genes *Ctla4*, *Casp3*, and *Il2ra* (CD25). To further examine this coordinate downregulation, we examined the expression pattern of genes in AM9, an acute effector module, across both acute and chronic infection (Figure 2D). We likewise visualized the expression pattern of genes

in the chronic effector module CM5. Compared to the protracted expression pattern of the genes of the acute module AM9 during chronic infection, the genes from the CM5 module were abruptly downregulated after the effector phase during acute infection. Thus, the transcriptional machinery underlying the effector phase of $CD8^+$ T cell differentiation appears to remain active for longer during chronic viral infection despite the known termination of the effector expansion and initiation of the contraction (Badovinac et al., 2002; Wherry et al., 2003). Together, these observations suggest that the temporal dynamics of module regulation could be a key feature of the development of memory versus exhaustion.

Network Topology Identifies Changes in Transcriptional Circuits in Acute Versus Chronic Infection

The network models developed here provide an opportunity to examine gene connectivity patterns that might provide insight into differential utilization of specific genes and pathways. This approach compares the difference in intramodular connectivity of a particular gene between the acute and chronic networks relative to the maximally connected gene in each network (Fuller et al., 2007). We used a network topology statistic and a measure of differential expression (Welch's *t*-statistic) to segregate genes based on changes in connectivity versus changes in expression (Figure 3A). The genes closer to the center of the plots in Figure 3A exhibit little change in either expression or connectivity. Because genes with low variance were filtered out prior to network creation, the genes at the center of these plots likely represent those similarly involved in $CD8^+$ T cell differentiation during acute versus chronic LCMV infection. In contrast, the peripheral sectors identify genes that have a change in connectivity, a change in expression, or both (Table S4). A lower connectivity score in either network implies that the gene in question has fewer interactions with other genes and is predicted to be less centrally involved in the module or network (Luscombe et al., 2004).

Genes with similarly preserved functionality can be located in the central sector at all time points (e.g., perforin and interferon-γ), indicating that these genes do not change in connectivity or expression between the two networks. Conversely, *Pdcd1* (PD-1) and *Il-7r* (CD127) are examples of genes with distinct roles in the $CD8^+$ response to acutely resolved or chronic infection. In addition to the higher expression of *Pdcd1* during chronic infection, PD-1 is also more highly connected in the chronic network at all time points (shifted to the left in Figure 3A). In contrast, though expression of *Il7r* (CD127) was initially higher in chronic infection at d6 p.i., *Il7r* progressively becomes more highly expressed following acute infection as these cells become IL-7-dependent memory T cells. *Il7r* is also more highly connected in the acute network (shifted to the right in Figure 3A). These two examples indicate how, independent of fold-change, connectivity may be used to identify genes whose function might change in different settings. Selected differentially connected genes are listed in Figure 3B.

We next investigated how the number of genes in each sector changed over time (Figure 3C). Sectors containing genes more highly expressed during acute infection (sectors 1, 7, and 8) showed a decline in the number of genes at d8, relative to d6, consistent with d8 marking a "disarming" point during acutely resolved infection. The genes highly expressed in an acute setting at d15 and d30 include known markers of $CD8^+$ T cell memory such as *Il7r* and *Cd44* (Table S4). For sectors containing genes more highly expressed during chronic infection (sectors 3, 4, 5), the number of genes peaks at d15, suggesting this as a key time point. At d15, for example, these sectors include the inhibitory receptors PD-1 (*Pdcd1*), *Lag3*, *Cd160*, Tim3 (*Havcr2*), and 2B4 (*Cd244*) as well as *Batf* and Blimp-1 (*Prdm1*), two transcription factors associated with exhaustion (Quigley et al., 2010; Shin et al., 2009).

We next segregated genes to identify potential differentially regulated pathways. Here, rather than using the DAVID tool used above, which only analyzes unranked gene sets, we used GOrilla to examine the set of genes ranked by differential connectivity. Genes more connected in the acute network were highly enriched for functions such as DNA replication and repair and cell cycle (Figure 3D). Driving this enrichment was a collection of genes in sectors 1, 2, and 3 that included growth factors, components of DNA repair processes, mediators of cell cycle control, E2F family transcription factors, and others (Table S5). Genes more highly connected in the chronic network (sectors 5, 6, and 7) were enriched for immune-related functions and the regulation of apoptosis and programmed cell death (Table S5). Contained in these sectors are cytokines, transcription factors, and inhibitory receptors, all of which lead to this enrichment pattern. Sector 5 genes were both more highly expressed and connected during chronic infection and included exhaustion-related genes such as *Cd160* and *Batf*. Thus, a direct comparison between the memory- and exhaustion-specific transcriptional networks revealed genes and pathways of differential prominence during acute versus chronic infection.

Coherent Expression of Transcription Factors in $CD8^+$ T Cell Memory Versus Exhaustion

We next sought to identify the transcription factor connectivity underlying $CD8^+$ T cell differentiation during acute versus chronic infection. We therefore defined separate networks restricted to just the 242 transcription factors that were contained in the original network described above (Figure 4A). These transcriptional circuits display expression patterns mirroring those of the greater coexpression networks, again with a prominent upregulation at effector time points (Figure 4B).

To examine the interconnected nature of acute and chronic transcription factor modules (ATM and CTM respectively), we examined temporal kinetics of each module eigengene (Figure 4B; Figure S4). These analyses identified transcription factor modules biased to the early phase of each infection (ATM2, ATM6, CTM1) or later memory versus exhaustion time points (ATM1, ATM3; CTM3, respectively). Of note are two acute transcription factor modules that were elevated in naive $CD8^+$ T cells, declined upon activation, and were re-expressed in memory: ATM3 and ATM4. Included in ATM4 are *Foxp1* and *Klf2*, two transcription factors with roles in T cell quiescence (Feng et al., 2011; Kuo et al., 1997) (Table S6), though the precise role of *Klf2* in quiescence versus trafficking might be more complex (Takada et al., 2011). During chronic infection, this pattern was observed for CTM4, despite the lack of a module with a corresponding profile in the whole-gene chronic network. Of the transcription factors in CTM4, the majority was also found

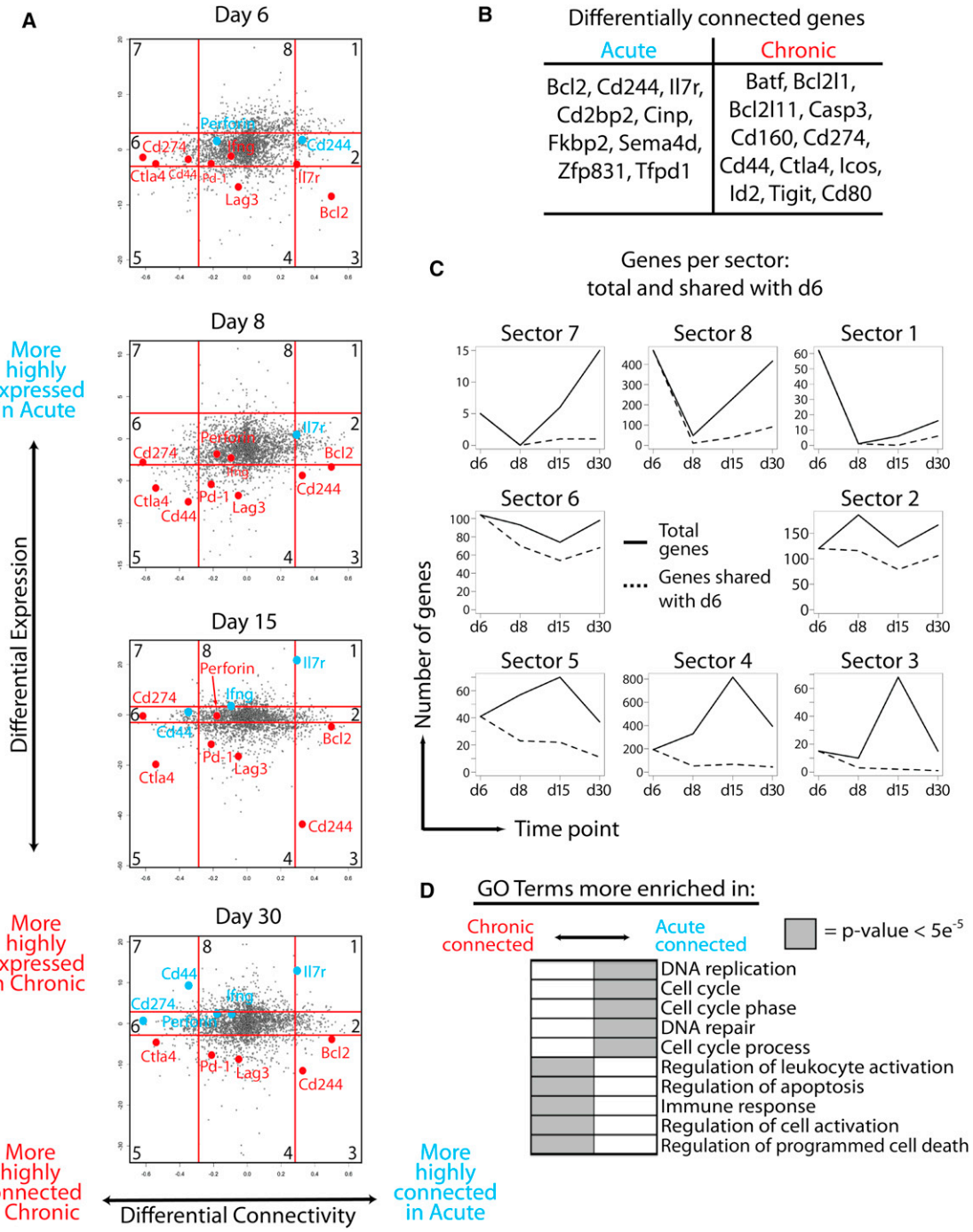

Figure 3. Differential Connectivity Versus Differential Expression for Genes in CD8$^+$ T Cells from Acutely Resolved Versus Chronic Infection

(A) Differential expression at d6, d8, d15, and d30 p.i., represented by Welch's t-statistic, is plotted against differential connectivity. Positive or negative differential connectivity scores represent an acute or chronic bias, respectively. Sectors are demarcated at t-statistics of ± 3 and at differential connectivity of ± 0.285. Selected genes are identified at all time points (Table S4).

(B) Genes in sectors 1, 2, and 3 and sectors 5, 6, and 7 known to be important in T cell biology are listed.

(C) For each time point (d6, d8, d15, and d30 p.i.), the number of genes per sector was quantified and longitudinally plotted (solid line). The number of genes common between a sector at d6 p.i. and that sector at all time points postinfection was plotted (dashed line).

(D) Differential connectivity reveals functional distinction. We used GOrilla (http://cbl-gorilla.cs.technion.ac.il/), to calculate overrepresented GO terms (http://www.geneontology.org) at both the positive and negative ends of the differential connectivity spectrum. A selected list of terms with p value < 5e^{-5} was visualized (Table S5).

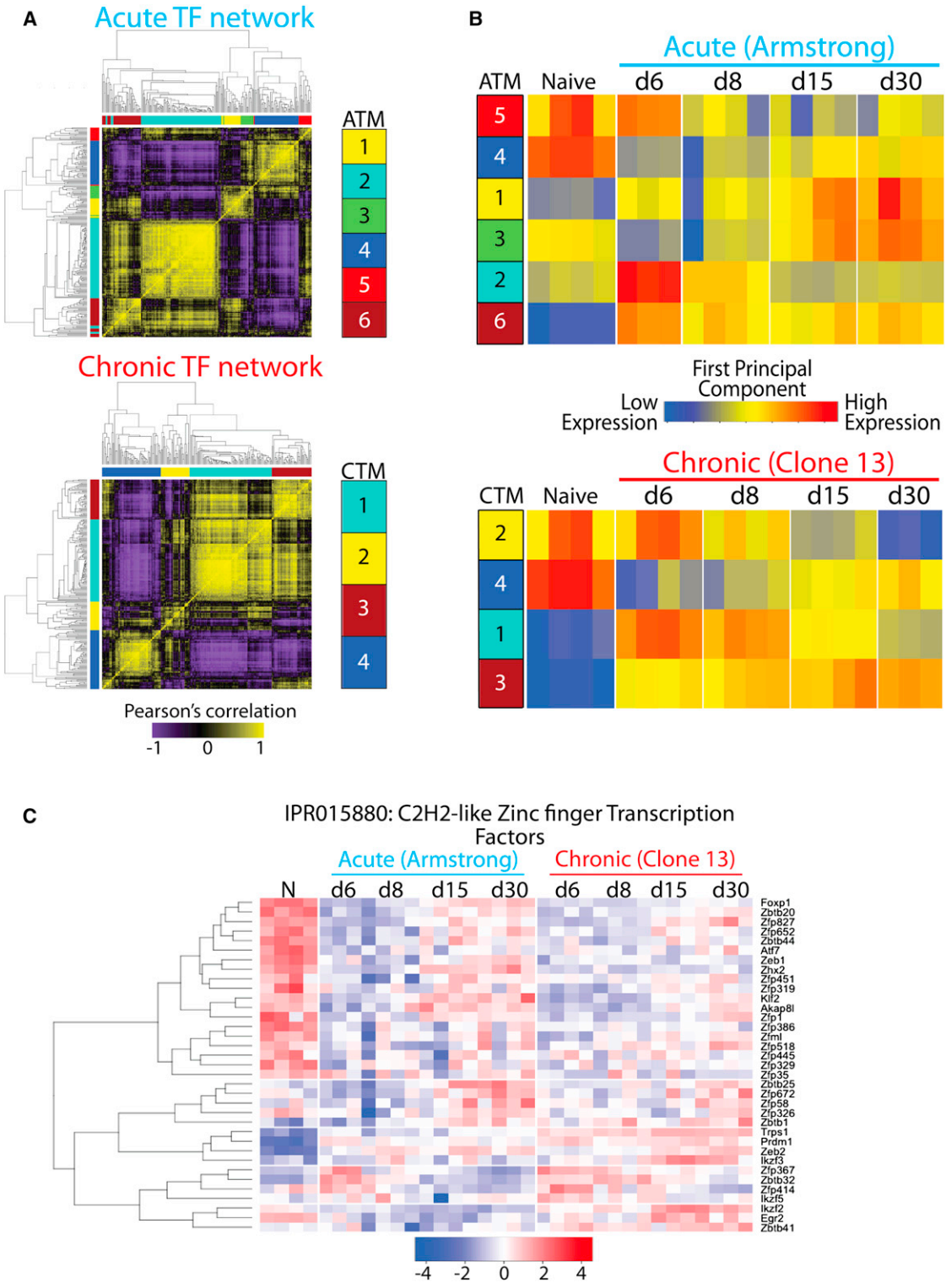

Figure 4. Transcription Factor Subnetworks Have Dynamically Expressed Modules

(A) Transcription factor-specific networks for 242 transcription factors were generated and modules identified as described above. Yellow and purple represent positive and negative correlations, respectively.

(B) The module eigengene was calculated as in Figure 2B and was used to hierarchically cluster modules. The expression of these module eigengenes was plotted; blue indicates low relative expression and red indicates high relative expression.

(C) Transcription factors assigned to the InterPro (http://www.ebi.ac.uk/interpro/) family "IPR015880: C2H2-like Zinc finger" were identified and visualized as a heatmap. Blue and red represent low and high relative expression, respectively.

in acute modules ATM3 and ATM4 with the notable exceptions of *Eomes*, *Ikzf2*, and *Egr2*.

Given the progressive functional differences between exhausted and memory CD8$^+$ T cells, there was an unexpected level of reuse of transcriptional circuitry. The high degree of preservation and the lack of an ''exhaustion specific'' transcription factor implied that exhausted CD8$^+$ T cells use many of the same transcription factors used during acute infection (Figure S2). The acute transcription factor module 6 (ATM6) and the chronic transcription factor module 3 (CTM3), for example, show a considerable overlap including several transcription factors central to the differentiation of effector, memory, and exhausted CD8$^+$ T cells, including T-bet (*Tbx21*), *Batf*, *Stat3*, and Blimp-1 (*Prdm1*). However, whereas ATM6 becomes upregulated following activation and maintains a steady state level of expression, the expression of CTM3 continues to rise over time. This observation is consistent with recent studies demonstrating that high expression of Blimp-1 fostered aspects of CD8$^+$ T cell exhaustion, whereas moderate Blimp-1 expression is required for effector functions and viral control (Shin et al., 2009). We also explored whether any transcription factor families exhibited family-wide differential expression and identified memory or exhaustion biased patterns for the C2H2-like zinc finger family (Interpro: IPR015880, Figure 4C). This family includes transcription factors with known T cell functions like Blimp-1 (*Prdm1*) and *Foxp1*, and those with uncharacterized roles in T cells, like *Zeb2* and *Trps1*, which provide interesting targets for future study.

Differential Connectivity of Transcription Factors in Acute and Chronic Infection

The modular reuse of many transcription factors suggested that some could have distinct functions during acute versus chronic infections. We therefore identified the most highly coexpressed ''neighbors'' for the 242 transcription factors from the acute and chronic coexpression networks. Many transcription factors had a large set of neighbors in common between both networks. In contrast, other transcription factors were connected to largely independent sets of genes (Figure 5A, Table S7). Eomesodermin (*Eomes*), in particular, was among the transcription factors with the lowest percentage of overlapping neighbors between networks. 2B4 (*Cd244*), a costimulatory or coinhibitory receptor highly expressed on exhausted CD8$^+$ T cells, was the only gene found to be common among the top 150 neighbors of *Eomes* (Figure 5A). This can be contrasted with T-bet (*Tbx21*), a transcription factor showing higher (~40% overlap) neighborhood concordance between acute and chronic settings (Figure 5A).

As a complimentary approach, we generated a ''difference network'' (Southworth et al., 2009) where connections between genes measure how dissimilar the connectivity pattern between gene pairs is in the acute and chronic settings. In this difference network, we can identify connections between pairs of genes that are similar in both networks, preserved in the acute but not the chronic network (blue lines in Figure 5B) or vice versa (red lines in Figure 5B). We defined difference networks for transcription factors as well as for all genes (Figure 5B; Figure S6). The HMG-box transcription factor *Tox* was identified as the most highly connected hub gene (indicated by node size); such central prominence in this difference network is consistent with Figure 5A demonstrating that *Tox* is differentially connected in acutely resolved and chronic infection. Though *Tox* has a role in development of many lymphoid lineages (Aliahmad et al., 2010), its role in CD8$^+$ T cells in the periphery during infection is unclear. This approach also identified receptor transport protein 4 (*Rtp4*), an interferon responsive gene, as potentially playing a distinct role in memory versus exhaustion (Figure S6). Additionally, *Eomes* was validated by this approach as having discrete coexpression neighborhoods in the acute versus chronic networks. Other genes of potential interest identified by this approach include *Ikzf2*, *Zbp1*, *Lass6*, *Rel*, and *Ifit3*.

To further explore transcription factor differential connectivity, we examined the gene neighbors of Eomes and T-bet. The acute neighbors of *Eomes* were effector-biased genes and many were involved in cell cycle processes and DNA replication (DAVID, p value < 0.05; Figure 5D). The chronic neighbors of *Eomes*, in contrast, became progressively more upregulated over time and were involved in the immune response, cytokine activity, and CD8$^+$ T cell differentiation (DAVID, p value < 0.05; Figure 5D). In contrast, the gene neighbors of T-bet included both context-independent neighbors and those specific to either the acute or chronic network (Figures 5C and 5D). The common set of T-bet neighbors had highly concordant patterns of expression (Figure S3). Similar observations were made for other transcription factors from Figure 5A (Figure S5). These results suggest that key transcription factors can be connected to distinct gene neighbors in different contexts.

We previously found that PD-1 expression distinguishes subsets of exhausted CD8$^+$ T cells that are either highly exhausted and terminal (PD-1^{Hi}) or that retain the ability to be reinvigorated by PD-1 blockade (PD-1^{Int}). T-bet is differentially expressed in these PD-1^{Hi} and PD-1^{Int} subsets (Blackburn et al., 2008; Kao et al., 2011). To test whether the acute or chronic neighbors of T-bet were differentially associated with these two distinct CD8$^+$ T cell subsets, we took advantage of a separate gene expression data set generated by our laboratory for sorted PD-1^{Int} and PD-1^{Hi} H-2D^b GP33-specific CD8$^+$ T cells 30 days p.i. with LCMV clone 13 (unpublished data). We performed gene set enrichment analysis (GSEA, [Subramanian et al., 2005]) on the PD-1^{Int} and PD-1^{Hi} exhausted CD8$^+$ T cell gene expression profiles by using the acute and chronic neighbors of T-bet defined in Figure 5C, because we predicted that the more reversible PD-1^{Int} subset might retain a signature of CD8$^+$ T cells from acute infection related to T-bet function. The genes connected with T-bet only during acute infection were strongly enriched toward the PD-1^{Int} profiles (Figure 6A). In contrast, the neighbors of T-bet from a chronic infection were more strongly enriched in the PD-1^{Hi} profiles (Figure 6A). Driving the enrichment of the acute neighbors of T-bet toward the PD-1^{Int} subset were *Klrg1*, *Il-18r1*, *Rora*, *Cd80*, and *Cd44*; alternatively, the leading edge of the chronic neighbors biased toward the PD-1^{Hi} subset includes *Lag3*, *Ctla4*, *Tigit*, *Batf*, and *Trps1*. These observations provide proof of principle for correlating network analysis-defined signatures with a biological phenotype in an independent data set. One possible alternative explanation, however, was that acute neighbors of any transcription factor would enrich toward the PD-1^{Int} signatures whereas chronic neighbors would be biased toward the PD-1^{Hi} profiles. To test this possibility, we used the sets of acute and chronic neighbors of all 242 transcription factors in Figure 4 and examined the enrichment of these

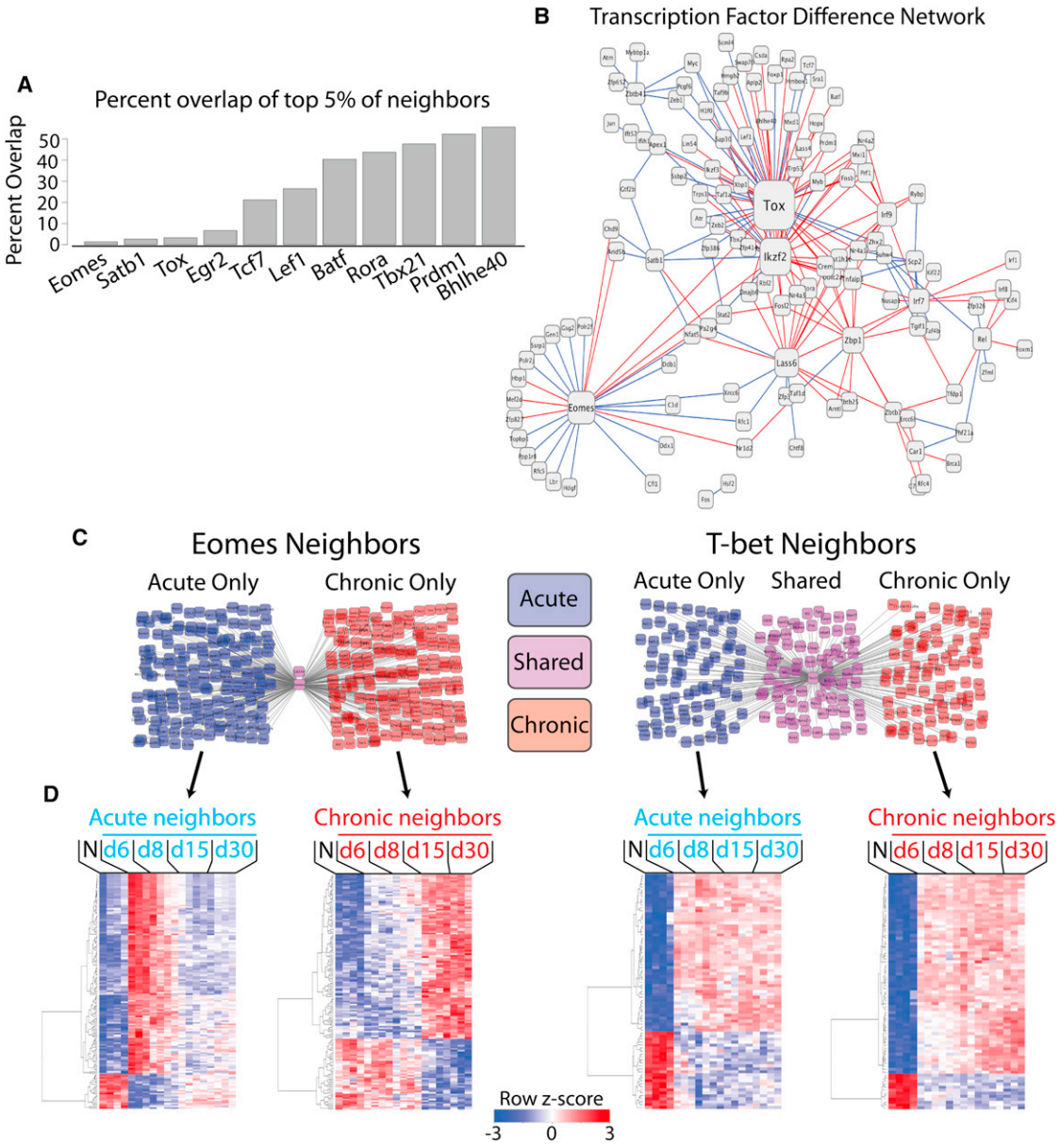

Figure 5. Acutely Resolved Versus Chronic Networks Differ in Transcription Factor Coexpression Relationships

(A) Genes were ranked by coexpression with each transcription factor. The top 150 (5% of total network) genes in the acute and chronic networks were retrieved and the percentage of genes that had preserved connections for each transcription factor in acute versus chronic infection was calculated (Table S7).

(B) Gene-gene edge scores from the transcription factor-specific chronic network were subtracted from the corresponding score in the acute network, as described (Southworth et al., 2009) to generate a difference network. Blue edges represent higher coexpression in the acute network, and red edges indicate higher coexpression in the chronic network. Number of connections per transcription factor is represented by node size.

(C) Genes plotted in red and blue are unique to the top 150 neighbors of the acute and chronic networks, respectively; purple identifies genes common to both sets of neighbors. *Eomes* or *Tbx21* are at the center of the left or right plot, respectively.

(D) Neighbors unique to either the acute or chronic network were identified, hierarchically clustered and visualized as heatmaps. Blue and red represent low and high relative expression, respectively.

sets of genes toward either the PD-1^{Int} or PD-1^{Hi} profiles. Although T-bet was not alone in having acute and chronic neighbors that respectively enriched in the PD-1^{Int} and PD-1^{Hi} subsets, there were many transcription factors whose neighbors did not follow this pattern (Figure 6B). Whereas other transcription factors whose gene connectivity patterns were similar to T-bet included *Prdm1* (Blimp-1) and *Bhlhe40*, the chronic neighbors of *Eomes*, *Batf*, and several STATs enriched more toward the PD-1^{Int} (Figure 6B). These observations suggest that individual transcription factors could have important context-specific functions but that these changes in context-specific regulation do not occur uniformly for all transcription factors.

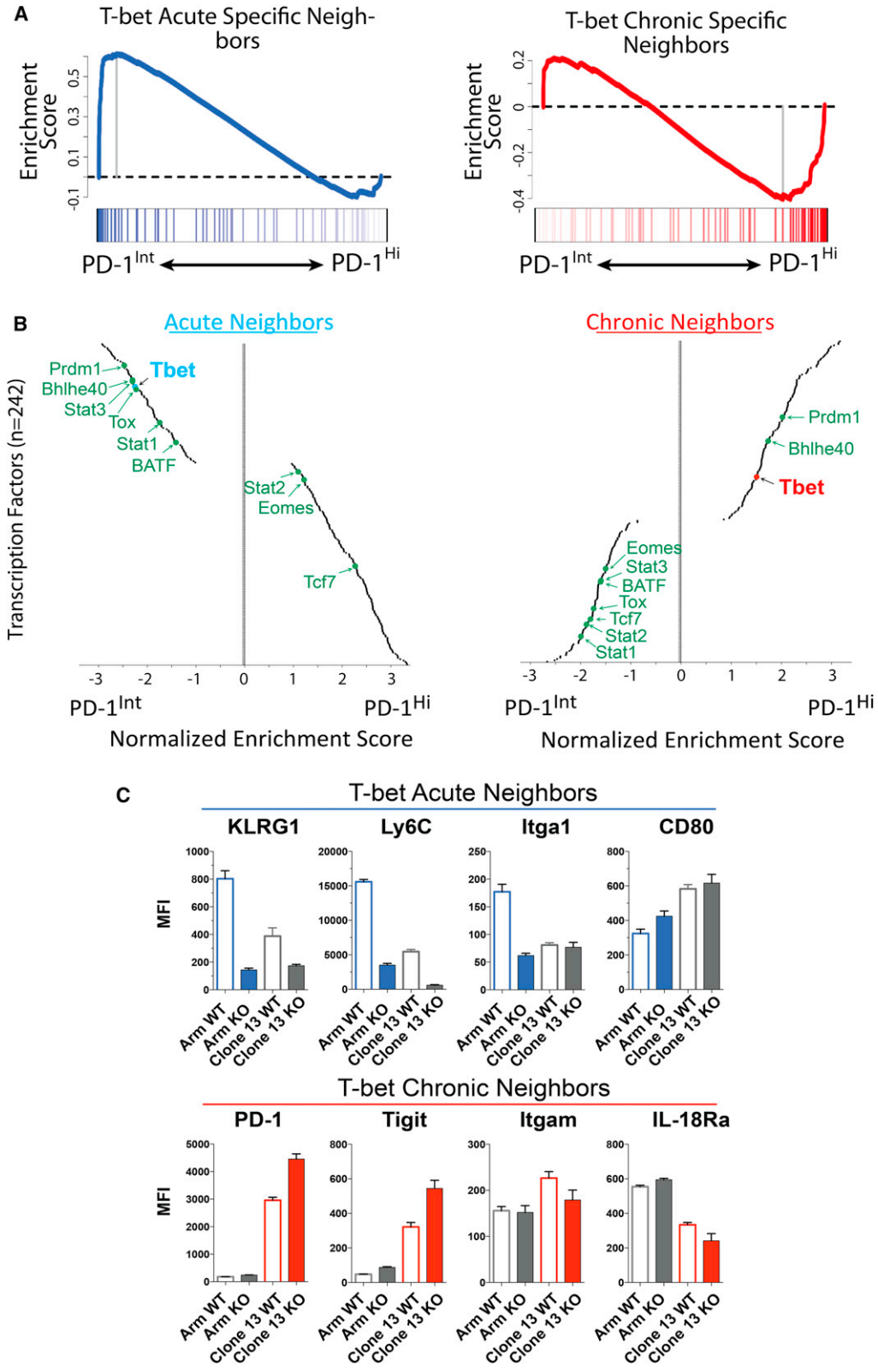

Figure 6. Validation of Context-Specific Functions Predicted for T-bet

(A) Context-specific T-bet neighbors bias transcriptional signatures from PD-1-defined subsets of exhausted CD8$^+$ T cells. Using the neighbors of T-bet from Figure 6B, we performed GSEA to compare profiles of PD-1^{int} versus PD-1^{hi} LCMV-specific CD8$^+$ T cells. The acute T-bet neighbors were strongly enriched in the PD-1^{int} data set (p value < 0.0001), whereas the chronic neighbors were more enriched toward PD-1^{hi} (p value = 0.01757).

As a proof of principle, we next tested specific predictions for individual gene neighbors of T-bet by flow cytometry in WT and T-bet-deficient CD8$^+$ T cells (Figure 6C). We predicted that the expression of the acute neighbors of T-bet would be more impacted by loss of T-bet during acute infection and vice versa for the chronic neighbors. We examined four acute neighbors, *Klrg1*, *Ly6C*, *Itga1*, and *Cd80*. Expression of these proteins was more impacted by T-bet deficiency during acute compared to chronic infection (Figure 6C). In contrast, the chronic neighbors *Pdcd1* (PD-1), *Tigit*, *Itgam*, and *Il18ra* were more impacted by T-bet deficiency during chronic infection. It is worth noting that these genes included those whose expression was positively regulated by T-bet (*Klrg1*, *Ly6C*, *Itga1*, *Itgam*, *Il18ra*) and some that were repressed by T-bet (*Cd80*, *Pdcd1* [PD-1] and *Tigit*). These analyses implicate T-bet as a central factor regulating the differentiation of exhausted versus memory CD8$^+$ T cells and provide direct evidence for differential function of T-bet in exhausted and memory CD8$^+$ T cells as predicted by the networks.

DISCUSSION

Exhausted CD8$^+$ T cells have a transcriptional profile profoundly different from memory CD8$^+$ T cells (Wherry et al., 2007). CD8$^+$ T cell exhaustion results in widespread functional defects, leading to impaired immunity in animal models and humans. Previous studies defined genes upregulated or downregulated during exhaustion (Wherry et al., 2007) leading to the discovery of individual molecules including inhibitory receptors (PD-1, LAG-3, etc. [Wherry, 2011]) and transcription factors (T-bet, Blimp-1, and Batf; see Kao et al., [2011]; Shin et al., [2009]; Quigley et al., [2010]). However, it has been challenging to define which genes are most important in the difference between exhaustion and memory. We used transcriptional network analysis to begin to define which genes and biological pathways were central to CD8 T cell exhaustion. This approach revealed several key insights distinguishing these two developmental programs. These include the absence of a clear module of quiescence in exhausted CD8$^+$ T cells, a framework for understanding the distinction between a prolonged activation program and a prolonged effector phase during exhaustion and the identification of biological pathways and hub genes involved in exhaustion (e.g., DNA repair, chromatin biology, zinc finger transcription factors, Wnt signaling, Bcl2 family members, *Rtp4*, and transcription factors including *Foxp1*, *Ikzf2*, *Zeb2*, *Lass6*, *Tox*, and *Eomes*). In addition, a fundamental feature of key transcription factors involved in CD8$^+$ T cell exhaustion, including T-bet, was specific and distinct context-dependent functions in acute versus chronic infection. Thus, in addition to providing a framework for investigating pathways involved in CD8$^+$ T cell exhaustion and revealing insights into the biology of T cell exhaustion, these studies demonstrate that specific transcription factors can be reused differently in distinct developmental programs in T cells.

Recent work has shown a widespread reuse of transcriptional programs between cell lineages that share a common hematopoietic stem cell (Novershtern et al., 2011). The studies presented here extend this notion of reuse of transcriptional circuits to CD8$^+$ T cells from acute versus chronic infection. For example, modules involved in the effector program and T cell activation were used during both acute and chronic infection at early time points. During acute infection, these modules were downregulated after the first week. In contrast, during chronic infection, a failure to return to quiescence was associated with preserved expression of activation molecules despite downregulation of effector modules. This split between modules that sustain expression and those that do not highlights intriguing possibilities. Modulating genes implicated in the prolonged activation program offers the potential to force exhausted CD8$^+$ T cells to "rest," and possibly restore memory differentiation or possibly to target missing effector modules to regain functionality. These observations also suggest that exhausted CD8$^+$ T cells are not simply (poorly) sustained effectors.

A set of insights from the current study stems from our identification of hub genes central to each network, including transcription factors, which would not have been identified using previous approaches. For example, when combined with differential expression, differential connectivity predicts important roles for several transcription factors previously unexamined in T cell exhaustion including: Helios (*Ikz2*), *Tox, Tcf7*, *Irf4, Irf7*, and *Zeb2*. Moreover, the network analyses predicted that major hub transcription factors such as Blimp-1 (*Prdm1*), T-bet (*Tbx21*), and Eomes might have distinct functions during acute versus chronic infection. Context-specific function has been reported for lineage-defining transcription factors, including concentration-dependent control of hematopoiesis by PU.1 (Laslo et al., 2006) and SMAD proteins imparting context specificity on developmental transcription factors such as MyoD, C/EBPα, and Oct4 (Mullen et al., 2011; Trompouki et al., 2011). Our previous studies suggested distinct roles in exhaustion versus memory for Blimp-1 as well as T-bet (Shin et al., [2009]; Kao et al., [2011]), but the mechanisms for these context-dependent functions were unclear. We now provide key predictions for how transcription factors such as Blimp-1, Eomes, and T-bet play distinct roles in acute versus chronic infection via interactions with different sets of genes. Further, we provide validation for regulation of distinct targets by T-bet in acute versus chronic infection. One additional implication of these observations is that the control of cell fate decisions might not always require a lineage specific transcription factor if, as is the case for *Eomes*, *Tox* and others, specific transcription factors can have almost completely distinct transcriptional interactions in different settings. Together, these observations suggest that the approach outlined here can provide a platform for future studies on the role of specific hub genes in CD8$^+$ T cell memory versus exhaustion.

Several other unappreciated predictions about the biology of memory and exhausted CD8$^+$ T cells were revealed in this

(B) Gene sets of context-specific neighbors for all 242 transcription factors were compared between the PD-1^{Int} versus PD-1^{hi} data set using GSEA.
(C) Flow cytometric analysis of context-specific neighbors of T-bet using T-bet deficient T cells. The expression of selected acute or chronic neighbors of T-bet was examined by flow cytometry on WT versus T-bet deficient DbGP33-specific CD8$^+$ T cells responding to acute or chronic LCMV infection at d30 p.i.. Error bars represent SD.

work. For example, although the Wnt-*Tcf7* pathway is important throughout T cell biology, the current analysis suggests an unexpected role for coordinated Wnt signaling during exhaustion. *Tcf7*, a key Wnt pathway transcription factor, is downregulated in exhausted CD8$^+$ T cells (Wherry et al., 2007). Thus, although many other genes are involved in Wnt signaling, the enriched connectivity of this pathway during exhaustion was unexpected. *Tcf7* activation by Wnt signaling can induce *Eomes* in memory CD8$^+$ T cells (Zhou et al., 2010); however, it is unknown whether *Tcf7* also has a role in exhausted CD8$^+$ T cells. The differential connectivity observed here for both *Eomes* and *Tcf7* raises the possibility that "neighbors" of these transcription factors could be important for context-dependent functions of the Wnt pathway.

The association of DNA repair pathways with memory CD8$^+$ T cells in the current studies was also unexpected. Thus, one possible feature distinguishing memory CD8$^+$ T cell development from exhaustion is proper maintenance of the genome. One prediction is that many rounds of cell division coupled with inefficient DNA repair are linked to T cell dysfunction, an idea that should be directly testable. The p53 and DNA damage response pathways have recently been linked with expression of Toll-like receptors on human T lymphocytes (Menendez et al., 2011), suggesting a possible connection between DNA stressors and immunity. Moreover, DNA damage was also found to be associated with tumor infiltrating T cells using genomic approaches (Baitsch et al., 2011). Further studies perturbing DNA repair and examining the impact on memory and exhaustion should allow direct testing of the predicted importance of DNA repair pathways.

Together, these results illustrate a complex and dynamic patterns of gene expression for CD8$^+$ T cells during acutely resolved versus chronic infection and provide insights to the developmental processes underlying each response. Our findings provide a resource for future examination of memory versus exhausted CD8$^+$ T cells and provide potential insights into pathways that could be targets for intervention and highly relevant for predicting the efficacy of vaccine-induced responses.

EXPERIMENTAL PROCEDURES

Animals and Infections

Female C57BL/6 mice (4–6 weeks old) were purchased from the Jackson Laboratories (Bar Harbor, Maine). Mice were infected with 2×10^5 pfu of LCMV Armstrong intraperitoneally or 2×10^6 pfu of LCMV clone 13 intravenously, as described (Wherry et al., 2003). Viral titers were performed by plaque assay as described (Wherry et al., 2003). All mice were used in accordance with Institutional Animal Care and Use Committee guidelines for the Wistar Institute and the University of Pennsylvania.

Cell Isolation, Sorting, and Flow Cytometry

Lymphocytes were isolated and MHC class I peptide tetramers were generated and used as previously described (Wherry et al., 2003). Naive CD44^{lo} CD8$^+$ T cells were isolated and sorted from uninfected C57BL/6 mice. H2-D^b GP33-specific CD8$^+$ T cells were sorted using MHC-I tetramers at d6, 8, 15, and 30 p.i. with either LCMV Arm or LCMV clone 13. PD-1^{int} and PD-1^{hi} exhausted CD8$^+$ T cells were isolated from mice 30 days p.i. with LCMV clone 13. All sorts were performed on a FACSAria (BD Bioscience). All samples were maintained at 4°C for the duration of the sort, 100,000 cells were collected, and sort purity was >95% for all populations. All antibodies were obtained from BD Biosciences, eBioscience, or Biolegend. A LSR II (BD ImmunoCytometry Systems) was used for flow cytometry, and data were analyzed with FlowJo 9.0.1 software (Treestar).

Microarray Data Acquisition and Processing

Total RNA was isolated from sorted CD8$^+$ T cells using TRIzol (Invitrogen, Carlsbad, CA). RNA was processed, amplified, labeled, and hybridized to Affymetrix GeneChip MoGene 1.0 st microarrays (Santa Clara, CA) by the University of Pennsylvania Microarray facility. Affymetrix Power Tools were used to process and quantile normalize fluorescent hybridization signals using Robust Multichip Averaging (Irizarry et al., 2003). Transcripts were $\log_2$ normalized. Outlier arrays were identified and excluded using an interarray correlation threshold (Oldham et al., 2008). Further filtering by expression and variance thresholds, set at $\mu > 5$ and $\sigma^2 > 0.15$, respectively, resulted in 3005 transcripts.

Microarray Analysis

The ClassNeighbors module of GenePattern was used to rank genes by the signal-to-noise ratio and identify class-biased genes (Reich et al., 2006). Significance Analysis of Microarrays and Gene Set Enrichment Analysis were performed on PD-1^{int} and PD-1^{hi} exhausted CD8$^+$ T cell arrays as described (Subramanian et al., 2005).

Weighted Coexpression Network Construction

Weighted gene coexpression network analysis was used to construct transcriptional coexpression networks (Langfelder and Horvath, 2008). A coexpression network was defined as a set of nodes, each representing a single transcript, and a set of edges, each equal to the Pearson's correlation coefficient (PCC) between the expression profiles of two transcripts. The adjacency transformation $A = r^\beta$ then scales the distribution of edge weights to fit the edge distribution of a scale-free network (Zhang and Horvath, 2005). Though other metrics (e.g., Spearman rank correlation, biweighted midcorrelation) exist, PCC was used for consistency with previous studies (Langfelder and Horvath, 2008). Acute and chronic transcriptional networks were generated from the gene expression profiles of virus-specific CD8$^+$ T cells responding to LCMV Armstrong or LCMV clone 13. The topological overlap metric and a dynamic tree-cutting algorithm were used to identify gene modules (Yip and Horvath, 2007). The 242 genes that both passed initial filtering criteria and were annotated by the GO term "DNA binding" are here referred to as transcription factors. The same methods as for the all-gene network (above) were used to generate transcription factor-specific networks and analyses. These and all following analyses were performed using R (Gentleman et al., 2004).

Modular Analysis

Fisher's Exact Test used to assess the significance of overlap between modules as described (Langfelder et al., 2011). Temporal expression profiles were summarized by module eigengenes (ME). Pearson's correlation coefficient between MEs was calculated and used to hierarchically cluster modules (Langfelder and Horvath, 2007). A one-way ANOVA was used to distinguish early from late expressed modules. Hub genes were identified and ranked by intramodular connectivity, as defined (Zhang and Horvath, 2005). Lists of hub genes were uploaded to the Database for Annotation, Visualization and Integrated Discovery (http://david.abcc.ncifcrf.gov/), (Huang et al., 2009b) to calculate significantly over-enriched Gene Ontology terms (http://www.geneontology.org).

Differential Connectivity

We defined differential connectivity as the difference between intramodular connectivity in the acute network, scaled relative to the maximally connected gene in that network, and intramodular connectivity in the chronic network, similarly scaled. Welch's two-sample t test was used as a measure of differential expression for each gene between the acute and chronic arrays from the same time point. GOrilla analysis for overenriched GO terms in a ranked list was performed (Eden et al., 2009).

Context-Specific Neighbor Identification

The adjacency score ($A = r^\beta$) was used to identify the most highly coexpressed "neighbors" to a given gene; we then identified the number and percentage of the top 150 neighbors common between the acute and chronic networks for each transcription factor (Langfelder and Horvath, 2008). Difference network

analysis was performed as described previously (Southworth et al., 2009). All network graphs were produced using Cytoscape.

Statistical Analyses

Welch's two-sample t test was used to calculate t-statistics in R (Gentleman et al., 2004). Fisher's exact test was used to identify overlap between modules and also by DAVID to identify enriched GO terms (Langfelder et al., 2011). GOrilla was used to identify enriched GO terms in a ranked list by the minimum hypergeometric score (Eden et al., 2009). A one-way ANOVA was used to identify prominently early and late module expression. For all applicable statistical tests, a p value of 0.05 was the maximum threshold for significance.

ACCESSION NUMBERS

Microarray data sets are available through the Gene Expression Omnibus (GSE41867).

SUPPLEMENTAL INFORMATION

Supplemental Information includes six figures and seven tables and can be found with this article online at http://dx.doi.org/10.1016/j.immuni.2012.08.021.

ACKNOWLEDGMENTS

We thank the Wherry laboratory for helpful suggestions and feedback. We also thank Avinash Bhandoola, Mark Siracusa, and Michael Abt for comments and input. This work was supported by the National Institutes of Health (AI082630, AI083022, AI078897, and HHSN266200500030C to E.J.W.) and the Dana Foundation (E.J.W). E.J.W. has a patent licensing agreement on the PD-1 pathway.

Received: June 29, 2011
Accepted: August 6, 2012
Published online: November 15, 2012

REFERENCES

Aliahmad, P., de la Torre, B., and Kaye, J. (2010). Shared dependence on the DNA-binding factor TOX for the development of lymphoid tissue-inducer cell and NK cell lineages. Nat. Immunol. *11*, 945–952.

Angelosanto, J.M., Blackburn, S.D., Crawford, A., and Wherry, E.J. (2012). Progressive loss of memory T cell potential and commitment to exhaustion during chronic viral infection. J. Virol. *86*, 8161–8170.

Badovinac, V.P., Porter, B.B., and Harty, J.T. (2002). Programmed contraction of CD8(+) T cells after infection. Nat. Immunol. *3*, 619–626.

Baitsch, L., Baumgaertner, P., Devêvre, E., Raghav, S.K., Legat, A., Barba, L., Wieckowski, S., Bouzourene, H., Deplancke, B., Romero, P., et al. (2011). Exhaustion of tumor-specific $CD8^+$ T cells in metastases from melanoma patients. J. Clin. Invest. *121*, 2350–2360.

Barber, D.L., Wherry, E.J., Masopust, D., Zhu, B., Allison, J.P., Sharpe, A.H., Freeman, G.J., and Ahmed, R. (2006). Restoring function in exhausted CD8 T cells during chronic viral infection. Nature *439*, 682–687.

Blackburn, S.D., Shin, H., Freeman, G.J., and Wherry, E.J. (2008). Selective expansion of a subset of exhausted CD8 T cells by anti-PD-L1 blockade. Proc Natl Acad Sci USA *105*, 15016–15021.

Brahmer, J.R., Tykodi, S.S., Chow, L.Q., Hwu, W.J., Topalian, S.L., Hwu, P., Drake, C.G., Camacho, L.H., Kauh, J., Odunsi, K., et al. (2012). Safety and Activity of Anti-PD-L1 Antibody in Patients with Advanced Cancer. N. Engl. J. Med. *366*, 2455–2465.

Brooks, D.G., McGavern, D.B., and Oldstone, M.B. (2006). Reprogramming of antiviral T cells prevents inactivation and restores T cell activity during persistent viral infection. J. Clin. Invest. *116*, 1675–1685.

Brown, P.O., and Botstein, D. (1999). Exploring the new world of the genome with DNA microarrays. Nat. Genet. *21*(1, Suppl), 33–37.

Carlson, M.R., Zhang, B., Fang, Z., Mischel, P.S., Horvath, S., and Nelson, S.F. (2006). Gene connectivity, function, and sequence conservation: predictions from modular yeast co-expression networks. BMC Genomics *7*, 40.

Carter, S.L., Brechbühler, C.M., Griffin, M., and Bond, A.T. (2004). Gene co-expression network topology provides a framework for molecular characterization of cellular state. Bioinformatics *20*, 2242–2250.

Chaussabel, D., Quinn, C., Shen, J., Patel, P., Glaser, C., Baldwin, N., Stichweh, D., Blankenship, D., Li, L., Munagala, I., et al. (2008). A modular analysis framework for blood genomics studies: application to systemic lupus erythematosus. Immunity *29*, 150–164.

Dong, J., and Horvath, S. (2007). Understanding network concepts in modules. BMC Syst. Biol. *1*, 24.

Eden, E., Navon, R., Steinfeld, I., Lipson, D., and Yakhini, Z. (2009). GOrilla: a tool for discovery and visualization of enriched GO terms in ranked gene lists. BMC Bioinformatics *10*, 48.

Elo, L.L., Järvenpää, H., Oresic, M., Lahesmaa, R., and Aittokallio, T. (2007). Systematic construction of gene coexpression networks with applications to human T helper cell differentiation process. Bioinformatics *23*, 2096–2103.

Feng, X., Wang, H., Takata, H., Day, T.J., Willen, J., and Hu, H. (2011). Transcription factor Foxp1 exerts essential cell-intrinsic regulation of the quiescence of naive T cells. Nat. Immunol. *12*, 544–550.

Fuller, M.J., and Zajac, A.J. (2003). Ablation of CD8 and CD4 T cell responses by high viral loads. J. Immunol. *170*, 477–486.

Fuller, T.F., Ghazalpour, A., Aten, J.E., Drake, T.A., Lusis, A.J., and Horvath, S. (2007). Weighted gene coexpression network analysis strategies applied to mouse weight. Mamm. Genome *18*, 463–472.

Gentleman, R.C., Carey, V.J., Bates, D.M., Bolstad, B., Dettling, M., Dudoit, S., Ellis, B., Gautier, L., Ge, Y., Gentry, J., et al. (2004). Bioconductor: open software development for computational biology and bioinformatics. Genome Biol. *5*, R80.

Han, J.D., Bertin, N., Hao, T., Goldberg, D.S., Berriz, G.F., Zhang, L.V., Dupuy, D., Walhout, A.J., Cusick, M.E., Roth, F.P., and Vidal, M. (2004). Evidence for dynamically organized modularity in the yeast protein-protein interaction network. Nature *430*, 88–93.

Hertoghs, K.M., Moerland, P.D., van Stijn, A., Remmerswaal, E.B., Yong, S.L., van de Berg, P.J., van Ham, S.M., Baas, F., ten Berge, I.J., and van Lier, R.A. (2010). Molecular profiling of cytomegalovirus-induced human $CD8^+$ T cell differentiation. J. Clin. Invest. *120*, 4077–4090.

Huang, W., Sherman, B.T., and Lempicki, R.A. (2009b). Systematic and integrative analysis of large gene lists using DAVID bioinformatics resources. Nat. Protoc. *4*, 44–57.

Irizarry, R.A., Bolstad, B.M., Collin, F., Cope, L.M., Hobbs, B., and Speed, T.P. (2003). Summaries of Affymetrix GeneChip probe level data. Nucleic Acids Res. *31*, e15.

Jeong, H., Mason, S.P., Barabási, A.L., and Oltvai, Z.N. (2001). Lethality and centrality in protein networks. Nature *411*, 41–42.

Kaech, S.M., Hemby, S., Kersh, E., and Ahmed, R. (2002). Molecular and functional profiling of memory CD8 T cell differentiation. Cell *111*, 837–851.

Kao, C., Oestreich, K.J., Paley, M.A., Crawford, A., Angelosanto, J.M., Ali, M.A., Intlekofer, A.M., Boss, J.M., Reiner, S.L., Weinmann, A.S., and Wherry, E.J. (2011). Transcription factor T-bet represses expression of the inhibitory receptor PD-1 and sustains virus-specific CD8+ T cell responses during chronic infection. Nat. Immunol. *12*, 663–671.

Kuo, C.T., Veselits, M.L., and Leiden, J.M. (1997). LKLF: A transcriptional regulator of single-positive T cell quiescence and survival. Science *277*, 1986–1990.

Langfelder, P., and Horvath, S. (2007). Eigengene networks for studying the relationships between co-expression modules. BMC Syst. Biol. *1*, 54.

Langfelder, P., and Horvath, S. (2008). WGCNA: an R package for weighted correlation network analysis. BMC Bioinformatics *9*, 559.

Langfelder, P., Luo, R., Oldham, M.C., and Horvath, S. (2011). Is my network module preserved and reproducible? PLoS Comput. Biol. *7*, e1001057.

Laslo, P., Spooner, C.J., Warmflash, A., Lancki, D.W., Lee, H.J., Sciammas, R., Gantner, B.N., Dinner, A.R., and Singh, H. (2006). Multilineage transcriptional priming and determination of alternate hematopoietic cell fates. Cell *126*, 755–766.

Luscombe, N.M., Babu, M.M., Yu, H., Snyder, M., Teichmann, S.A., and Gerstein, M. (2004). Genomic analysis of regulatory network dynamics reveals large topological changes. Nature *431*, 308–312.

Menendez, D., Shatz, M., Azzam, K., Garantziotis, S., Fessler, M.B., and Resnick, M.A. (2011). The Toll-like receptor gene family is integrated into human DNA damage and p53 networks. PLoS Genet. *7*, e1001360.

Mullen, A.C., Orlando, D.A., Newman, J.J., Lovén, J., Kumar, R.M., Bilodeau, S., Reddy, J., Guenther, M.G., DeKoter, R.P., and Young, R.A. (2011). Master transcription factors determine cell-type-specific responses to TGF-β signaling. Cell *147*, 565–576.

Ng, S.Y., Yoshida, T., Zhang, J., and Georgopoulos, K. (2009). Genome-wide lineage-specific transcriptional networks underscore Ikaros-dependent lymphoid priming in hematopoietic stem cells. Immunity *30*, 493–507.

Novershtern, N., Subramanian, A., Lawton, L.N., Mak, R.H., Haining, W.N., McConkey, M.E., Habib, N., Yosef, N., Chang, C.Y., Shay, T., et al. (2011). Densely interconnected transcriptional circuits control cell states in human hematopoiesis. Cell *144*, 296–309.

Oldham, M.C., Konopka, G., Iwamoto, K., Langfelder, P., Kato, T., Horvath, S., and Geschwind, D.H. (2008). Functional organization of the transcriptome in human brain. Nat. Neurosci. *11*, 1271–1282.

Quigley, M., Pereyra, F., Nilsson, B., Porichis, F., Fonseca, C., Eichbaum, Q., Julg, B., Jesneck, J.L., Brosnahan, K., Imam, S., et al. (2010). Transcriptional analysis of HIV-specific CD8$^+$ T cells shows that PD-1 inhibits T cell function by upregulating BATF. Nat. Med. *16*, 1147–1151.

Reich, M., Liefeld, T., Gould, J., Lerner, J., Tamayo, P., and Mesirov, J.P. (2006). GenePattern 2.0. Nat. Genet. *38*, 500–501.

Shin, H., Blackburn, S.D., Intlekofer, A.M., Kao, C., Angelosanto, J.M., Reiner, S.L., and Wherry, E.J. (2009). A Role for the Transcriptional Repressor Blimp-1 in CD8($^+$) T Cell Exhaustion during Chronic Viral Infection. Immunity *31*, 309–329.

Southworth, L.K., Owen, A.B., and Kim, S.K. (2009). Aging mice show a decreasing correlation of gene expression within genetic modules. PLoS Genet. *5*, e1000776.

Subramanian, A., Tamayo, P., Mootha, V.K., Mukherjee, S., Ebert, B.L., Gillette, M.A., Paulovich, A., Pomeroy, S.L., Golub, T.R., Lander, E.S., and Mesirov, J.P. (2005). Gene set enrichment analysis: a knowledge-based approach for interpreting genome-wide expression profiles. Proc. Natl. Acad. Sci. USA *102*, 15545–15550.

Takada, K., Wang, X., Hart, G.T., Odumade, O.A., Weinreich, M.A., Hogquist, K.A., and Jameson, S.C. (2011). Kruppel-like factor 2 is required for trafficking but not quiescence in postactivated T cells. J. Immunol. *186*, 775–783.

Topalian, S.L., Hodi, F.S., Brahmer, J.R., Gettinger, S.N., Smith, D.C., McDermott, D.F., Powderly, J.D., Carvajal, R.D., Sosman, J.A., Atkins, M.B., et al. (2012). Safety, Activity, and Immune Correlates of Anti-PD-1 Antibody in Cancer. N. Engl. J. Med. *366*, 2443–2454.

Trompouki, E., Bowman, T.V., Lawton, L.N., Fan, Z.P., Wu, D.C., DiBiase, A., Martin, C.S., Cech, J.N., Sessa, A.K., Leblanc, J.L., et al. (2011). Lineage regulators direct BMP and Wnt pathways to cell-specific programs during differentiation and regeneration. Cell *147*, 577–589.

Wherry, E.J. (2011). T cell exhaustion. Nat. Immunol. *12*, 492–499.

Wherry, E.J., Blattman, J.N., Murali-Krishna, K., van der Most, R., and Ahmed, R. (2003). Viral persistence alters CD8 T-cell immunodominance and tissue distribution and results in distinct stages of functional impairment. J. Virol. *77*, 4911–4927.

Wherry, E.J., Ha, S.J., Kaech, S.M., Haining, W.N., Sarkar, S., Kalia, V., Subramaniam, S., Blattman, J.N., Barber, D.L., and Ahmed, R. (2007). Molecular signature of CD8$^+$ T cell exhaustion during chronic viral infection. Immunity *27*, 670–684.

Williams, M.A., and Bevan, M.J. (2007). Effector and memory CTL differentiation. Annu. Rev. Immunol. *25*, 171–192.

Wirth, T.C., Xue, H.H., Rai, D., Sabel, J.T., Bair, T., Harty, J.T., and Badovinac, V.P. (2010). Repetitive antigen stimulation induces stepwise transcriptome diversification but preserves a core signature of memory CD8($^+$) T cell differentiation. Immunity *33*, 128–140.

Yip, A.M., and Horvath, S. (2007). Gene network interconnectedness and the generalized topological overlap measure. BMC Bioinformatics *8*, 22.

Zhang, B., and Horvath, S. (2005). A general framework for weighted gene co-expression network analysis. Statistical applications in genetics and molecular biology *4*, Article 17.

Zhou, X., Yu, S., Zhao, D.M., Harty, J.T., Badovinac, V.P., and Xue, H.H. (2010). Differentiation and persistence of memory CD8($^+$) T cells depend on T cell factor 1. Immunity *33*, 229–240.